



ELSEVIER

Nuclear Instruments and Methods in Physics Research B 135 (1998) 82–86

NIM B
Beam Interactions
with Materials & Atoms

Measurements of soft X-rays in collision of slow multiply charged Ar ions with an amorphous C target

S. Ninomiya ^{a,*}, Y. Yamazaki ^a, T. Azuma ^a, K. Komaki ^a, K. Kuroki ^b, M. Sekiguchi ^c^a *Institute of Physics, University of Tokyo, Komaba 3-8-1, Meguro, Tokyo 153, Japan*^b *National Research Institute of Police Science, Chiyoda 100, Japan*^c *Center for Nuclear Study, School of Science, University of Tokyo, Tanashi 188, Japan*

Abstract

Soft X-rays were measured in collision of 1–3 keV/u Ar^{q+} ($q = 2–14$) ions on an amorphous C target. Ar L X-rays due to initial L-shell holes were successfully decomposed. It was found that L-shell vacancies of Ar were filled stepwise primarily via 3s–2p transition for each step. © 1998 Elsevier Science B.V.

PACS: 34.50.Dy*Keywords:* Hollow atoms; Multiply charged ions; X-ray emission

1. Introduction

The interaction between slow multiple charged ions (MCIs) and solids has been studied extensively for more than two decades [1–9]. When a slow MCI approaches a solid surface, target valence electrons are selectively captured into highly excited states. Such high multiple excited atom (ion) with open innershells is referred to as a “hollow atom in the first generation (HA1)”. Even if the initial velocity of the MCI toward the surface is very small, the HA1 eventually and inevitably hits the surface within a finite time because of the image acceleration. Part of HA1s then reach the surface

before relaxations to innershells, i.e., innershell holes could still be kept at or below the surface, which are referred to as “hollow atoms in the second generation”(HA2s). Previous studies of Auger electron and X-ray emissions are more or less related to this HA2. Recently, we have succeeded to study HA1s employing a microcapillary target [10,11].

To investigate the relaxation process of HA2 at and below the surface, observations of L (or M and outer shells) X-rays have several advantages [12] over those of K Auger electrons, which have been much more favored. The reasons are as follows; (1) X-rays have information on HA2 deeper inside a solid than Auger electrons due to their longer attenuation length, (2) data analyses of X-ray spectra are in general easier than those of Auger electron spectra because X-ray spectra are

* Corresponding author. Tel.: 81 3 5454 6515; fax: 81 3 3485 2904; e-mail: ninomiya@insac7.tanashi.kek.jp.

hardly distorted by inelastic collisions, and (3) L shell (or M and outer shells) is more useful than K shell because of the variety of the hole number.

We have measured L X-rays emitted from Ar^{q+} ($q = 7\text{--}14$) ions on Al and Be surfaces [12]. In the present report, we extend the X-ray measurements for an amorphous C target.

2. Experiment

The present study was performed using a HyperECR Ion Source [13] at Center for Nuclear Study (CNS), School of Science, University of Tokyo. MCIs from the ECR ion source were charge-state selected, collimated to a size of $1 \times 1 \text{ cm}^2$, and led to a target chamber. The angle between the surface and the beam was $\sim 70^\circ$. The target was biased at +9 V to prevent emission of slow secondary electrons. X-rays were measured with an open window Si(Li) detector, which viewed the collision region at 90° to the beam direction. Further experimental details are given elsewhere [12].

3. Results and discussions

The intensities of X-rays, $Y(q, E_k)$, in the Ar L X-ray energy region are shown in Fig. 1 for incident ion energies E_k of 40, 70 and 120 keV as a function of the incident charge state q . Even when Ar ions have no L shell hole initially ($q \leq 8$), rather strong X-rays were observed at $E_k = 120 \text{ keV}$, where the yield for Ar^{9+} is about 20% larger than that for Ar^{8+} . On the other hand, in the case of the Be target [12], the X-ray yield for Ar^{9+} ions is several times larger than that for Ar^{8+} . The yields increase considerably with respect to E_k for $2 \leq q \leq 7$, but do not depend so much on E_k for $q \geq 9$. With respect to q , it is seen that the yields roughly stay constant for $2 \leq q \leq 7$, and increase for $q \geq 9$. Slight increases observed at $q = 8$ may be due to the contribution from metastable states [12].

Fig. 2(a)–(g) shows the observed X-ray spectra, $dY(q, E_k)/dE$, for Ar^{q+} ($q = 7\text{--}14$) on the C target at $E_k = 40, 70$ and 120 keV . For $2 \leq q \leq 7$, not only the X-ray intensities but also spectral shapes (not

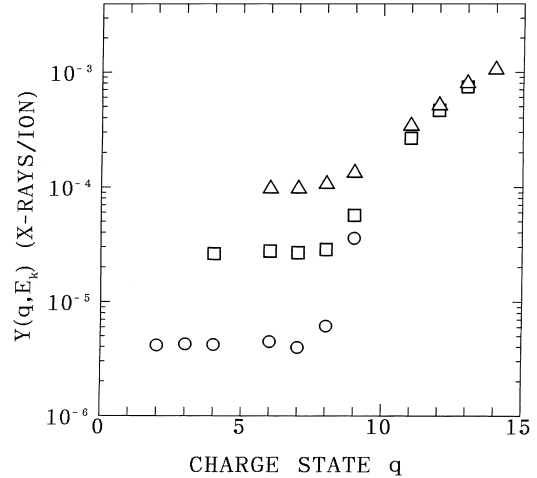


Fig. 1. X-ray yield $Y(q, E_k)$ for $E_k = 40 \text{ keV}$ (circle), 70 keV (square) and 120 keV (triangle) for Ar^{q+} on an amorphous C target as a function of q .

shown in Fig. 2) were found to be roughly the same with each other for each E_k . For $q \geq 9$, a bump was seen in the high energy side of the spectra, which eventually became the second peaks for $q = 13$ and 14 . These two-peak structures in the X-ray spectra were not observed for Al and Be targets [12].

As C KL X-rays are also expected to appear in the observed energy range (277 eV [14]), observed X-ray spectrum, $dY(q, E_k)/dE$, is decomposed as

$$\frac{dY(q, E_k)}{dE} = \frac{dY_p(q, E_k)}{dE} + \frac{dY_t(q, E_k)}{dE}, \quad (1)$$

where Y_p is the yield of X-rays emitted from the projectile (i.e. Ar L X-ray), Y_t is that from the target (i.e. C K X-ray) and E is the X-ray energy.

For Al and Be targets, within the energy range of Ar L X-rays (200–800 eV), the target X-rays are not expected, i.e. $dY(q, E_k)/dE = dY_p(q, E_k)/dE$. It was found that dY_p/dE consisted of two parts, i.e.,

$$\frac{dY_p(q, E_k)}{dE} = \frac{dY_{pn}(q)}{dE} + \frac{dY_{pe}(E_k)}{dE}, \quad (2)$$

where Y_{pn} is the yield of the Ar L X-rays emitted near the surface where the L-shell hole distribution is still in non-equilibrium, Y_{pe} is that emitted deep in the target where the equilibrium has already been reached [12]. It was assumed that Y_{pn} depend only on q and Y_{pe} depend only on E_k , respectively

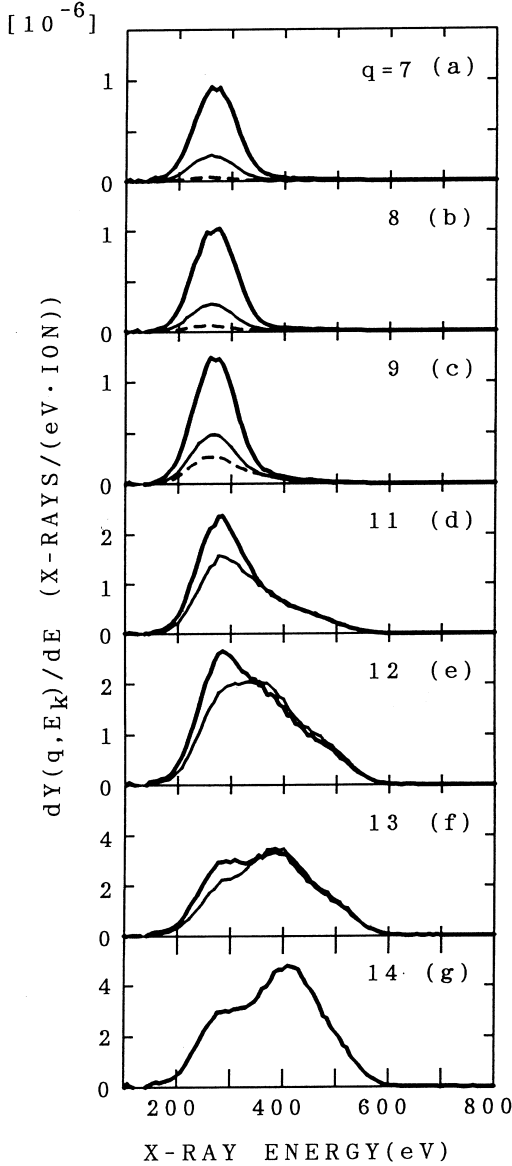


Fig. 2. X-ray spectra $dY(q, E_k)/dE$ for Ar^{q+} on an amorphous C target for $E_k = 40$ keV (dashed line), 70 keV (thin solid line) and 120 keV (thick solid line): (a) $q = 7$, (b) $q = 8$, (c) $q = 9$, (d) $q = 11$, (e) $q = 12$, (f) $q = 13$ and (g) $q = 14$.

(the expression of $Y_{\text{pn}}(q)$ means that the function Y_{pn} only depends on the specified argument q). In the region of L shell-hole non-equilibrium, inner-shell holes are filled one by one emitting an X-ray or an Auger electron at each step. Such a scenario allows to disintegrate $dY_{\text{pn}}(q)/dE$ into a

spectrum corresponding to each step. In other words, the spectrum, $dI_{\text{p}}(n_{\text{L}})/dE$, ($n_{\text{L}} = q - 8$) defined by

$$\begin{aligned} \frac{dI_{\text{p}}(n_{\text{L}})}{dE} &\equiv \frac{dY_{\text{pn}}(q)}{dE} - \frac{dY_{\text{pn}}(q-1)}{dE} \\ &= \frac{dY_{\text{p}}(q)}{dE} - \frac{dY_{\text{p}}(q-1)}{dE}, \end{aligned} \quad (3)$$

gives the energy distributions of X-rays emitted when the number of Ar L-shell holes changes from n_{L} to $n_{\text{L}} - 1$. The above procedure revealed that: (1) 3s–2p transitions were dominant in each step, (2) 3d–2p transitions were very weak for these targets and (3) contributions of transitions from higher principal quantum numbers like 4s–2p were discernible [12].

For a C target, difference spectra, $dI(n_{\text{L}}, E_k)/dE$, defined by

$$\begin{aligned} \frac{dI(n_{\text{L}}, E_k)}{dE} &\equiv \frac{dY(q, E_k)}{dE} - \frac{dY(q-1, E_k)}{dE} \\ &= \frac{dI_{\text{p}}(n_{\text{L}}, E_k)}{dE} + \frac{dI_{\text{t}}(n_{\text{L}}, E_k)}{dE}, \end{aligned} \quad (4)$$

would again be useful to consider the X-ray production processes, where $dI_{\text{t}}(n_{\text{L}}, E_k)/dE = dY_{\text{t}}(q, E_k)/dE - dY_{\text{t}}(q-1, E_k)/dE$. We will, for the sake of generality, keep E_k -dependence in the difference spectrum, i.e., $dI_{\text{p}}(n_{\text{L}}, E_k)/dE + dI_{\text{t}}(n_{\text{L}}, E_k)/dE$.

Fig. 3(a)–(e) show $dI(n_{\text{L}}, E_k)/dE$ for $n_{\text{L}} = 1$ –6 for $E_k = 40, 70$ and 120 keV bombarding the C target. Even though $dY(q, E_k)/dE$ for different E_k were quite different with each other for $q \geq 11$ (see Fig. 2(d)–(f)), $dI(n_{\text{L}}, E_k)/dE$ were similar to each other. In other words, the difference spectra had weak E_k -dependence, i.e.,

$$\frac{dI(n_{\text{L}}, E_k)}{dE} = \frac{dI(n_{\text{L}})}{dE} = \frac{dI_{\text{p}}(n_{\text{L}})}{dE} + \frac{dI_{\text{t}}(n_{\text{L}})}{dE}. \quad (5)$$

It should be noted that Eq. (5) supports our simple model on the relaxation of HA2 which was briefly discussed in the beginning of this section [12]. As seen in Fig. 3, $dI(n_{\text{L}})/dE$ were very small around the C KL X-ray energy (277 eV) at least for $n_{\text{L}} \geq 4$. For comparison, the peak energy of $dI(n_{\text{L}})/dE$ for a C target is similar to that for a Be target for all n_{L} . Therefore, we may conclude that $I(n_{\text{L}})$ consists primarily of Ar L X-rays and

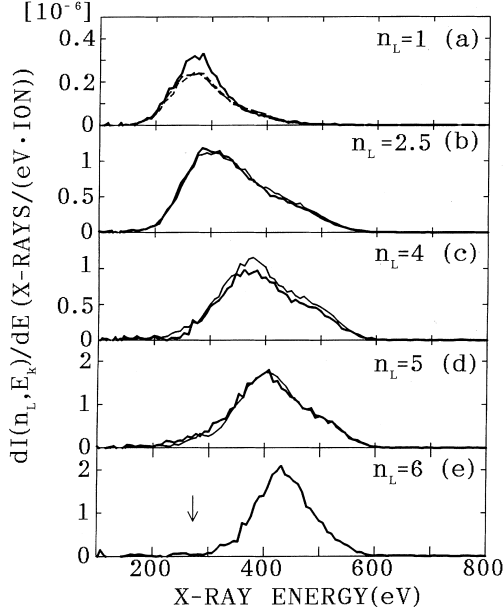


Fig. 3. $dI(n_L, E_k)/dE$ defined by Eq. (4) on an amorphous C target for $E_k = 40$ keV (dashed line), 70 keV (thin solid line) and 120 keV (thick solid line): (a) $n_L = 1$, (b) $n_L = 2.5$, (c) $n_L = 4$, (d) $n_L = 5$ and (e) $n_L = 6$. The arrow in Fig. 3(e) shows the C K L X-ray energy. The spectra for $n_L = 1$ were obtained from $dY(q=9, E_k)/dE - dY(q=7, E_k)/dE$ instead of $dY(q=9, E_k)/dE - dY(q=8, E_k)/dE$ to avoid the influence of metastable component of Ar^{8+} ions. The spectra for $n_L = 2.5$ is defined by $\{dY(q=11, E_k)/dE - dY(q=9, E_k)/dE\}/2$.

contains very weak contributions from C K X-rays, if any, i.e.,

$$\frac{dI(n_L)}{dE} = \frac{dI_p(n_L)}{dE}. \quad (6)$$

In this way, the observed X-rays, $dY(q, E_k)/dE$ for $q \geq 9$ were found to consist of three parts, i.e.,

$$\begin{aligned} \frac{dY(q, E_k)}{dE} &= \sum_{j=1}^{n_L} \frac{dI_p(j)}{dE} + \frac{dY_p(E_k)}{dE} + \frac{dY_t(E_k)}{dE} \\ &= \sum_{j=1}^{n_L} \frac{dI_p(j)}{dE} + \frac{dY(q=7, E_k)}{dE}. \end{aligned} \quad (7)$$

Peaks or bumps observed around 400 eV in $dY(q, E_k)/dE$ for $q \geq 11$ (see Fig. 2(d)–(g)) correspond to the first term in Eq. (7), i.e. Ar L X-rays originating from initial L shell holes. On the other hand, bumps or peaks observed around 300 eV in $dY(q, E_k)/dE$ are partly attributed to collisional

excitations, $dY(q=7, E_k)/dE$. However, further decomposition into $dY_p(E_k)/dE$ and $dY_t(E_k)/dE$ has not been made yet.

The peak energies of $dI_p(n_L)/dE$ on a C target were likely to be attributed to the 3s–2p transitions rather than the 3d–2p transitions for all n_L , the conclusion of which were again similar to the Be target case, though the peak energy are slightly higher than those for the Be target [12]. Contributions of transitions from higher principal quantum numbers like 4s–2p may be part of the reason of the peak shifts.

4. Conclusion

Soft X-rays were measured in collision of slow Ar^{q+} ions with a C target. Ar L X-ray spectra corresponding to the filling of initial L shell holes were evaluated, which were found to depend weakly on their kinetic energies. The L shell holes were filled stepwise primarily via 3s–2p transitions, which was similar to the case of Be target.

Acknowledgements

The research is supported by the Grant-in-Aid for Scientific Research on Priority Areas, Physics of Multiple Charged Ions (05238103) and by the Grant-in-Aid for Developmental Scientific Research (07555006) from the Ministry of Education, Science and Culture.

References

- [1] U.A. Arifov, É.S. Mukhamadiev, E.S. Parilis, A.S. Pas-yuk, Soviet Phys.-Tech. Phys. 18 (1973) 118.
- [2] D.M. Zehner, S.H. Overbury, C.C. Havener, F.W. Meyer, W. Heiland, Surf. Sci. 178 (1986) 359.
- [3] J.-P. Briand, L. de Billy, P. Charles, S. Essabaa, P. Briand, R. Geller, J.P. Desclaux, S. Bliman, C. Ristori, Phys. Rev. Lett. 65 (1990) 159.
- [4] J. Burgdörfer, P. Lerner, F.W. Meyer, Phys. Rev. A 44 (1991) 5674.
- [5] J. Das, L. Folkert, R. Morgenstern, Phys. Rev. A 45 (1992) 4669.
- [6] H. Winter, C. Auth, R. Schuch, E. Beebe, Phys. Rev. Lett. 71 (1993) 1939.

- [7] M. Grether, A. Spieler, R. Köhrbrück, N. Stolterfoht, *Phys. Rev. A* 52 (1995) 426.
- [8] J. Limburg, S. Schipper, R. Hoekstra, R. Morgenstern, H. Kurz, F. Aumayr, HP. Winter, *Phys. Rev. Lett.* 75 (1995) 217.
- [9] J.-P. Briand, S. Thuriiez, G. Giardino, G. Borsoni, M. Froment, M. Eddrich, C. Sébenne, *Phys. Rev. Lett.* 77 (1996) 1452.
- [10] Y. Yamazaki, S. Ninomiya, F. Koike, H. Masuda, T. Azuma, K. Komaki, K. Kuroki, M. Sekiguchi, *J. Phys. Soc. Jpn.* 65 (1996) 1199.
- [11] S. Ninomiya, Y. Yamazaki, F. Koike, H. Masuda, T. Azuma, K. Komaki, K. Kuroki, M. Sekiguchi, *Phys. Rev. Lett.* 78 (1997) 4557.
- [12] S. Ninomiya, Y. Yamazaki, K. Sawatari, M. Irako, K. Komaki, T. Azuma, K. Kuroki, M. Sekiguchi, *Nucl. Instrum. Method B* 115 (1996) 177.
- [13] M. Sekiguchi et al., *Proceedings of 12th International Conference on Cyclotrons and their Applications, Vancouver, World Scientific, 1992, p. 326.*
- [14] C.M. Lederer, V.S. Shirley, *Tables of Isotopes, Wiley/Interscience, 1978, Appendices-11.*